Experimental and Numerical Determination of Temperature Gradients for a Single Tube Alkali Metal Thermal-to-Electric Converter Cell

Author: Shonte Wright – Thermal Engineer
Jet Propulsion Laboratory, California Institute of Technology, Pasadena, CA

An Alkali Metal Thermal-to-Electric Converter (AMTEC) cell is an energy storage device under consideration by Jet Propulsion Laboratory-NASA (JPL-NASA) for future deep space missions (Figure 1). This apparatus is of particular interest to JPL due to its potential for long-term reliability and high conversion efficiency; additionally the cell is insensitive to orientation and devoid of moving parts, two attributes of tremendous importance for long-term missions. Although AMTEC has demonstrated potential, researchers continue to work towards optimizing its performance. Over the years, several different hot and cold end temperature combinations have been examined, however, the optimal combination has yet to be identified [2, 3, 5, 6].

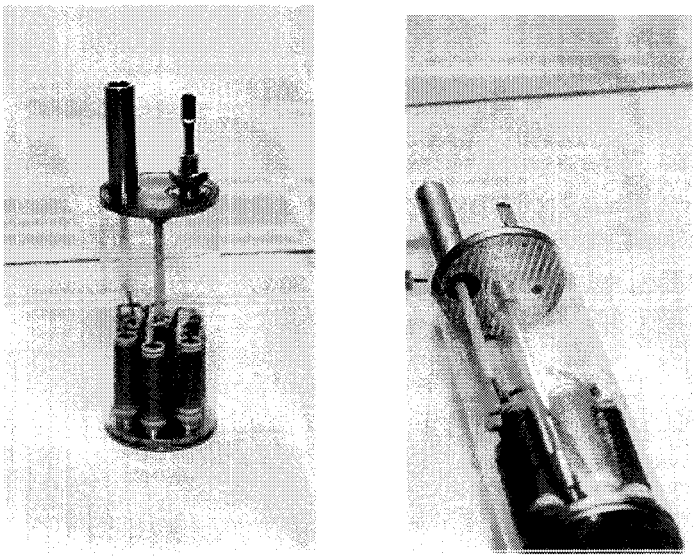

Figure 1. AMTEC cell depicted with a clear containment

This paper presents the results from the experimental and numerical determination of shell temperature gradients for a single tube AMTEC cell evaluated under simulated deep space operating conditions. The temperatures on the hot and cold ends of the cell, in the Beta Alumina Solid Electrolyte (BASE) tube, in the evaporator, and along the containment of the cell were experimentally obtained. By using the (experimentally obtained) hot and cold end temperatures, as boundary conditions, a numerical model was generated to calculate the temperatures along the cell containment for comparison. To

effectively replicate the experimental results, it was necessary to account for both radiative and convective heat transfer on the inner cell wall.

The AMTEC cell evaluated in this study was similar to the cell depicted in Figure 1, with the exception that it operated with only one BASE tube. The cell was evaluated experimentally under nine steady state temperature conditions, and the experimental data demonstrating the longest steady state periods was examined numerically. Prior to a more in depth look at the experimental and numerical analysis, a general operational description of the cell is offered.

The AMTEC cell operation cycle begins when heat is supplied to the hot (evaporator) end of the cell. Following the introduction of heat, liquid sodium travels down the (fine-pore) wick filled artery located in the center of the cell, through the evaporator section (where the liquid is vaporized), to the plenum base located at the hot end of the cell. Once the high-pressure sodium vapor reaches the plenum base it is equally distributed to each of the BASE tubes as depicted in Figure 2.

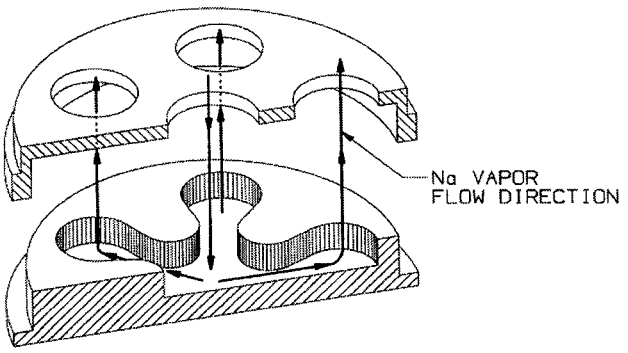

Figure 2. Illustration of the sodium vapor flow direction [8]

Upon entering each BASE tube, electrons are stripped from sodium atoms, and sodium ions diffuse through the BASE tubes, to the electrode (cathode) on the external surface of the BASE tube. The electrons stripped at the inner electrode are carried by conductors to power an external load. The electrons then return to the external electrode to recombine with the sodium ions diffusing through the BASE tube wall to form a low pressure sodium vapor outside the tube, which then travels to and condenses at the cold (condenser) end of the cell. The sodium is then wicked back to the hot (evaporator) end of the cell where it again evaporates in continuation of the cycle. As electronic current is drawn from the series connected BASE tubes, power is produced (Figure 3) [12]. A schematic illustrating the operation cycle is shown in Figure 4[1].

[1] Figure 4 illustrates a mechanical pump, however the current generation of AMTEC cells (like the one investigated in this study), rely on a wick and sodium surface tension to achieve the pressure differential between the hot and cold ends of the cell.

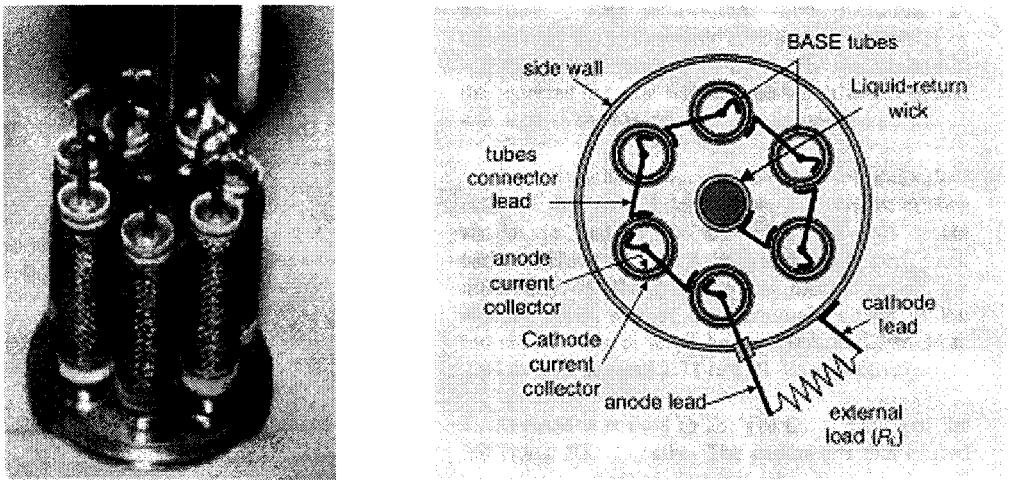

Figure 3. BASE tube connection to hot end, and diagrammed description [13, 10]

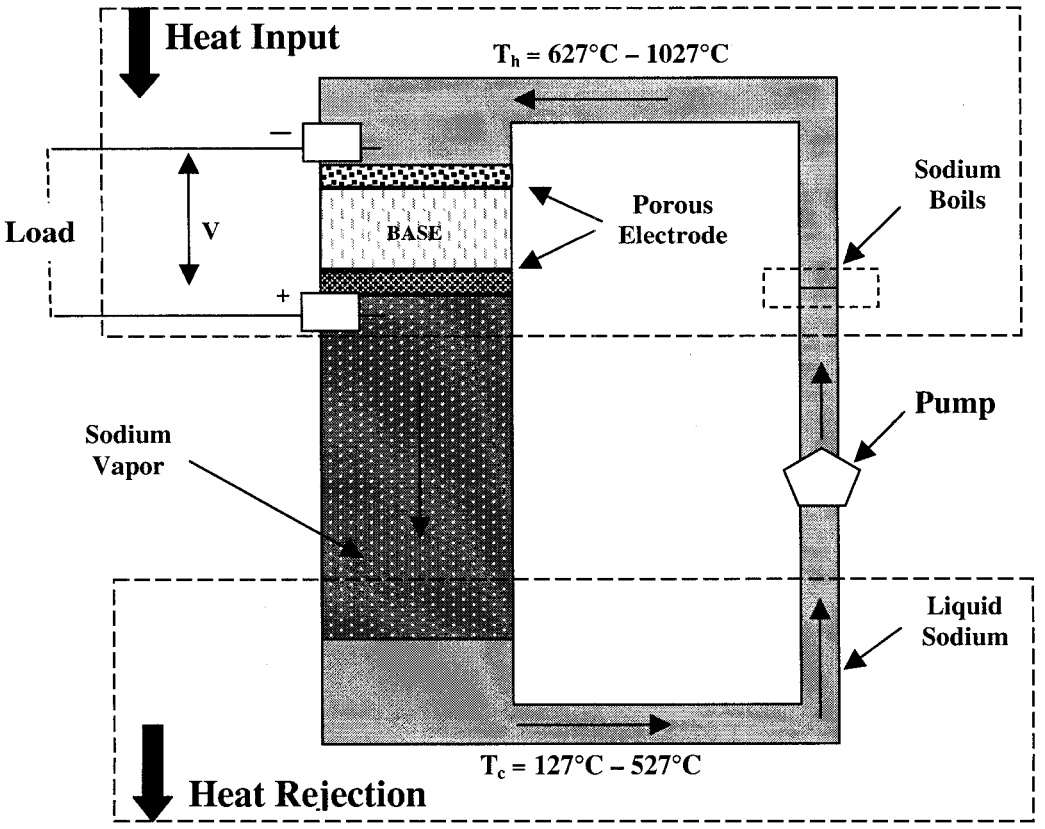

Figure 4. Schematic of AMTEC cell operation [11]

The experimental portion of the temperature gradient characterization was performed in a vacuum chamber in order to simulate the cell's operating environment. Following the preparation of the test set-up, thermocouples were positioned in and along the cell (Figures 5-6). Next, the cell was mounted terminal side down on a copper plate, and insulated in a radial direction using alternating concentric layers of Cerwool and molybdenum foil insulation. These layers of insulation were sandwiched between layers of microporous insulation. The entire insulation package was supported by a sheet metal plate held in place with nuts and washers symmetrically positioned along the four rods of a support structure at the bottom of the chamber (Figure 7).

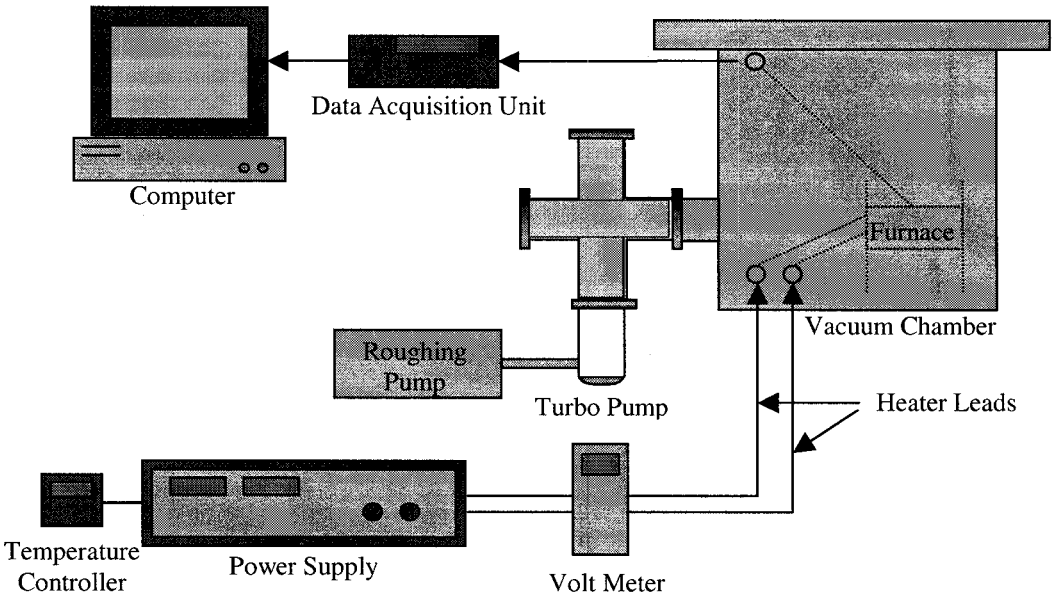

Figure 5. Test setup

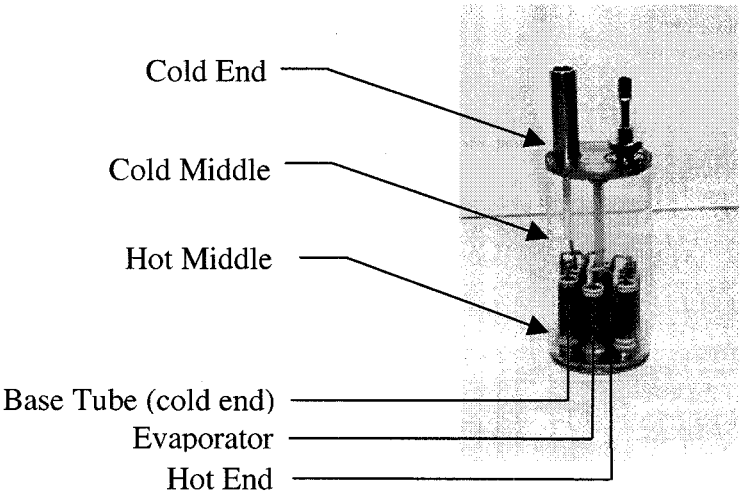

Figure 6. Temperature measurement locations in and along the cell

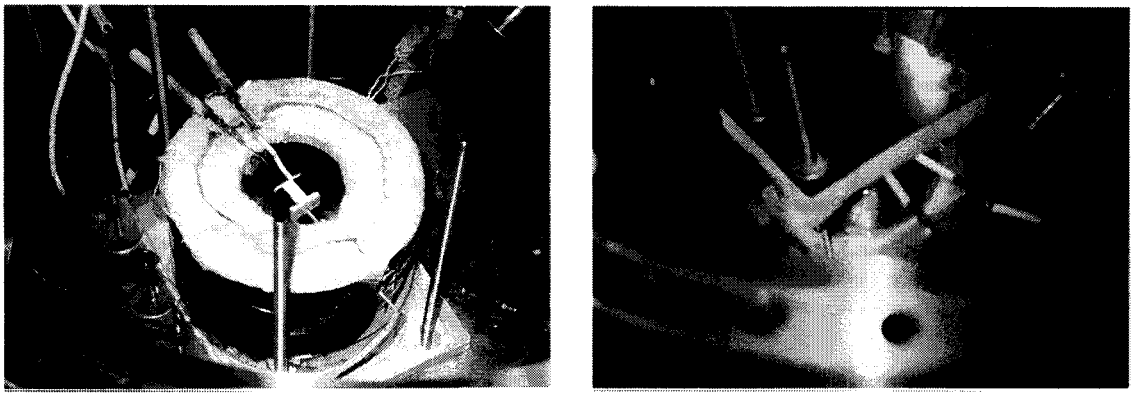

Figure 7. Concentrically layered insulation surrounding AMTEC cell with copper mounting plate held in place by threaded support rods (left); concentrically layered insulation and heater, secured in place by layers of Microtherm insulation and a thin sheet metal plate (right)

Over the course of 1300 hours, the hot end of the cell was ramped to the temperatures listed in Table 1, and allowed to soak (Figures 8-9). Throughout the experiment there were a few instrument malfunctions, however they were promptly repaired and steady state evaluation resumed. Of the nine steady state periods examined, those demonstrating the longest steady state periods were selected for numerical evaluation (Table 2).

Table 1. Experimental conditions examined

Hot End	Cold End
382°C	63°C
382°C	79°C
743°C	224°C
949°C	255°C
1301°C	338°C
940°C	277°C
917°C	265°C
925°C	266°C
930°C	267°C

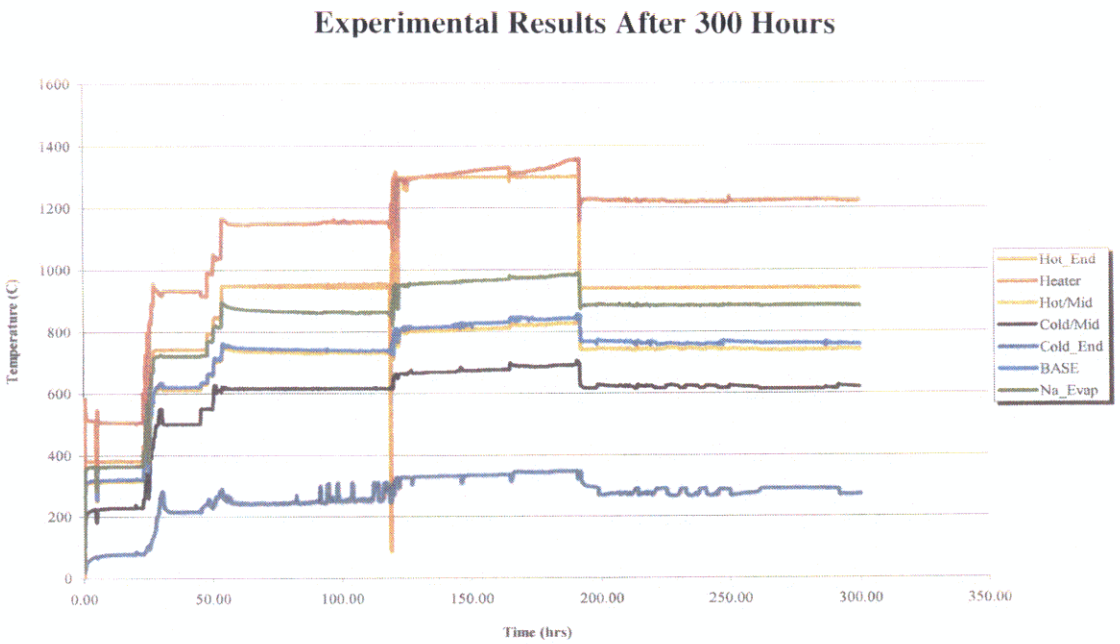

Figure 8. Experimental results after 300 hours

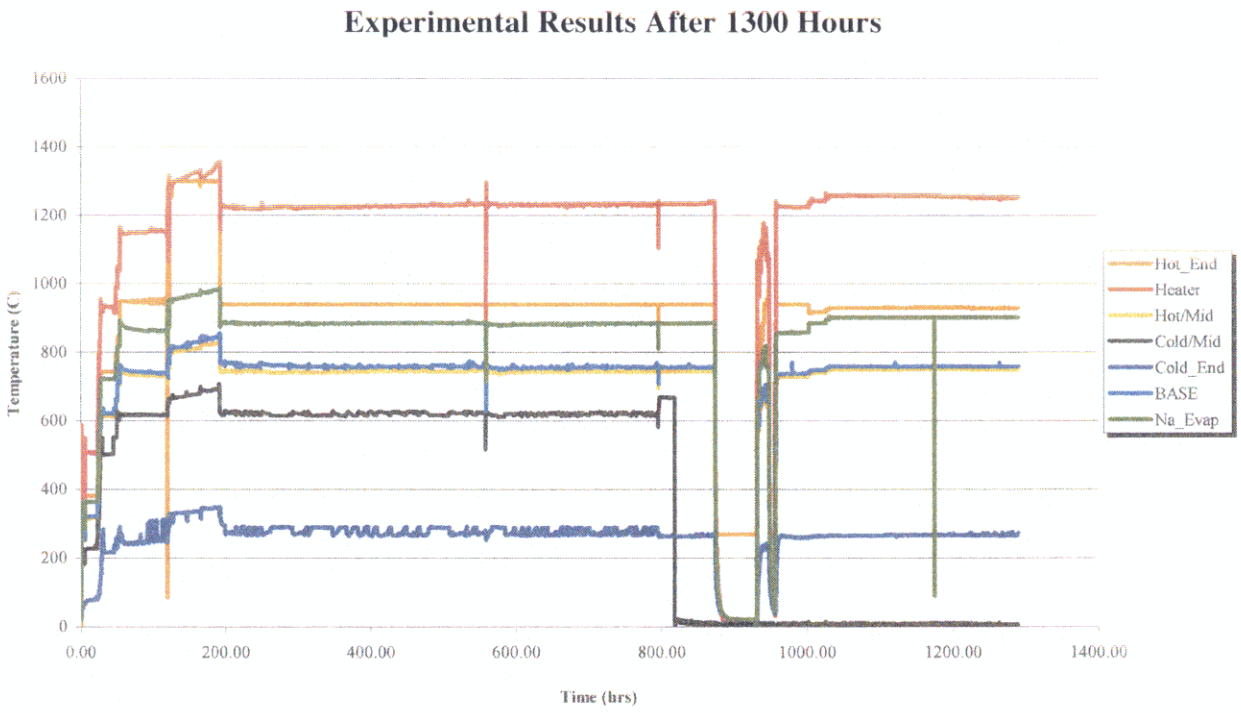

Figure 9. Experimental results after 1300 hours

Table 2. The boundary conditions considered in the numerical steady state evaluation

Hot End Temperature	Cold End Temperature
382°C	79°C
743°C	224°C
940°C	277°C

Heat was supplied to the evaporator end of the cell and was transferred along the cell containment (shell) by means of conduction, with radiative exchange occurring between the shell and a surrounding concentric cylinder of molybdenum foil, and between each component inside the cell. Conduction and radiation were the two methods of heat transfer initially considered in this model since convection was zero on the outer surface of the shell (due to the vacuum environment). Convection on the inner shell surface was originally assumed negligible in keeping with the thermal modeling work of earlier developers. However, the numerical results obtained under the assumption of negligible internal convection were inconsistent with the experimental data, and this led to further analysis of the flow regime on the cell interior. The mean free path of the sodium molecules was calculated according to:

$$\lambda = \frac{V}{\sqrt{2}N\pi d^2}$$

where: N/V = molecules per unit volume
d = molecular diameter of sodium

The number of molecules per unit volume, N/V was calculated by employing the ideal gas law:

$$PV = nR_u T$$

where: P = sodium vapor pressure
V = cell volume
n = number of moles of sodium
R_u = universal gas constant
T = evaporator temperature

and assuming the pressure to be the saturation pressure corresponding to the cold (condenser) end temperature.

Vapor pressures were determined from a plot of sodium pressure versus temperature using the cold end temperature under consideration (Figure 10). The mean free path, was used to determine the Knudsen number based on the cell inner diameter according to:

$$Kn = \frac{\lambda}{D}.$$

The Knudsen number was used to distinguish between the three flow regimes – continuum, slip flow, and free molecular flow. For Knudsen numbers above 4, free molecular flow conditions exist [8]; for Knudsen numbers below about 10^{-2} continuum flow conditions exist. Between these limits lies the transition or slip flow regime.

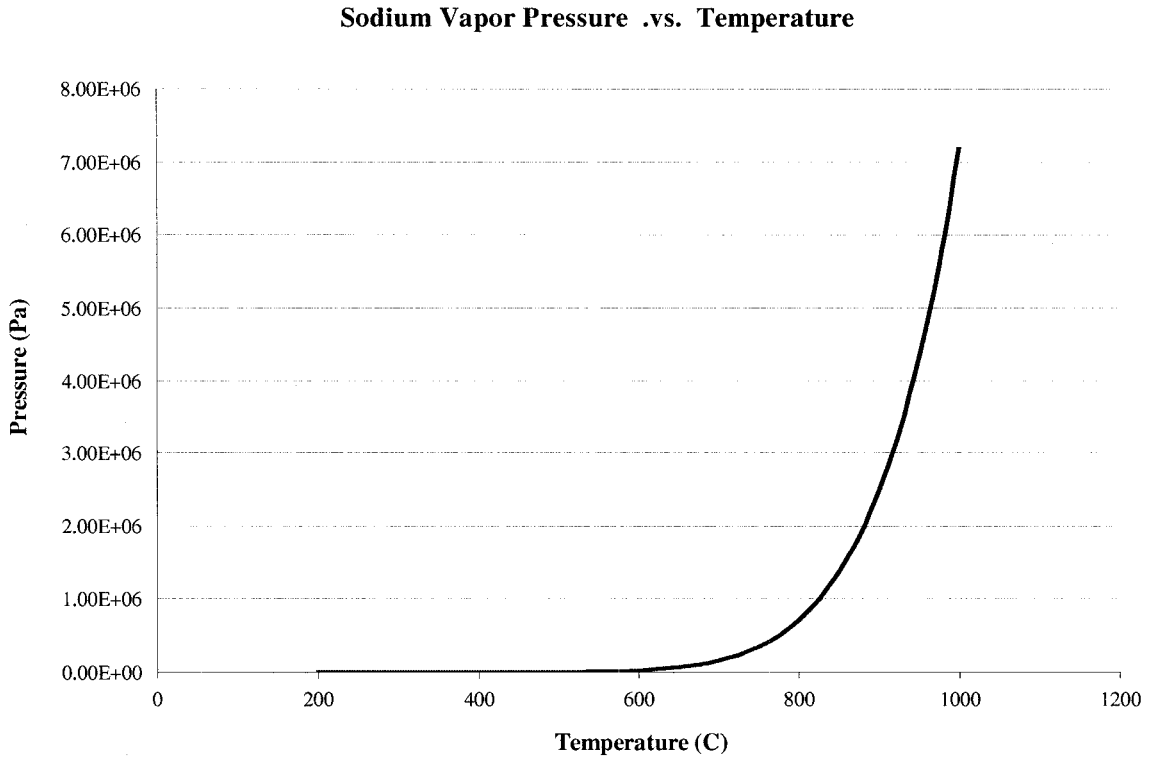

Figure 10. Sodium pressure versus temperature

In this instance the mean free path was calculated for cold end temperatures of 79°C, 224°C, and 277°C, and compared with the cell diameter to yield Knudsen numbers of 1.11 x 10^5, 2.431, and .2783 (respectively). For the cold end temperature of 79°C free molecular flow conditions were validated, however the Knudsen numbers calculated in the cold end cases of 224°C and 277°C support a slip flow condition. Since the Knudsen numbers calculated in each instance did not support the assumption of a non-convective

inner shell condition, a heat transfer coefficient and fluid temperature was assigned to the surface of the inner shell during numerical modeling. In the numerical model generated by Orbital Sciences Corporation (OSC) a slip flow condition at the inner shell surface was predicted and given consideration within the model [7, 9].

The numerical (thermal) modeling of the AMTEC cell was carried out using WinTherm, a general-purpose thermal modeling tool currently under development by ThermoAnalytics, Inc. The thermal model of the cell was constructed with shell geometry to include the cell containment, central wick, BASE tube, and the first molybdenum layer of the concentrically layered insulation (Figure 11).

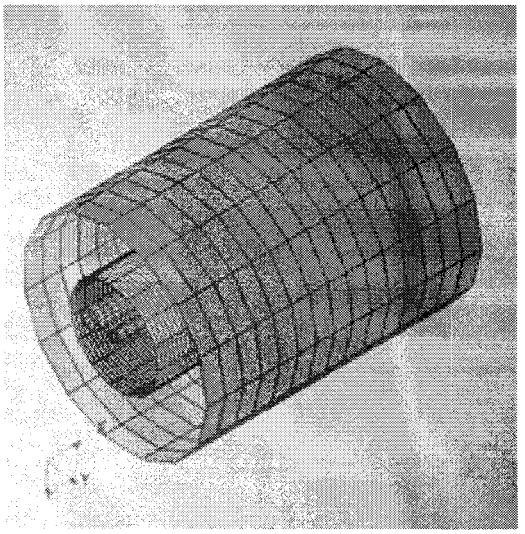

Figure 11. Thermal model displaying first molybdenum layer, cell containment, BASE tube, and wick

After the cell geometry and first layer of molybdenum foil were constructed, the material properties were assigned and boundary conditions were set. The external cell environment was set as non-convective (vacuum) and the inner cell containment was assigned a heat transfer coefficient. Temperature boundary conditions consistent with the operating conditions under consideration were assigned to the hot and cold ends of the cell. Additionally, the temperature recorded at the bottom (hot end) of the first molybdenum foil layer was incorporated into the model as an assigned temperature.

The steady state temperatures associated with the hot and cold end boundary conditions listed in Table 2 were examined numerically. As illustrated in Figures 12-14, the numerically generated values without consideration given to internal cell convection did not compare well with the experimentally obtained values. There were percent differences as high as 36%, suggesting that internal convection played a significant role in the heat transfer along the cell containment.

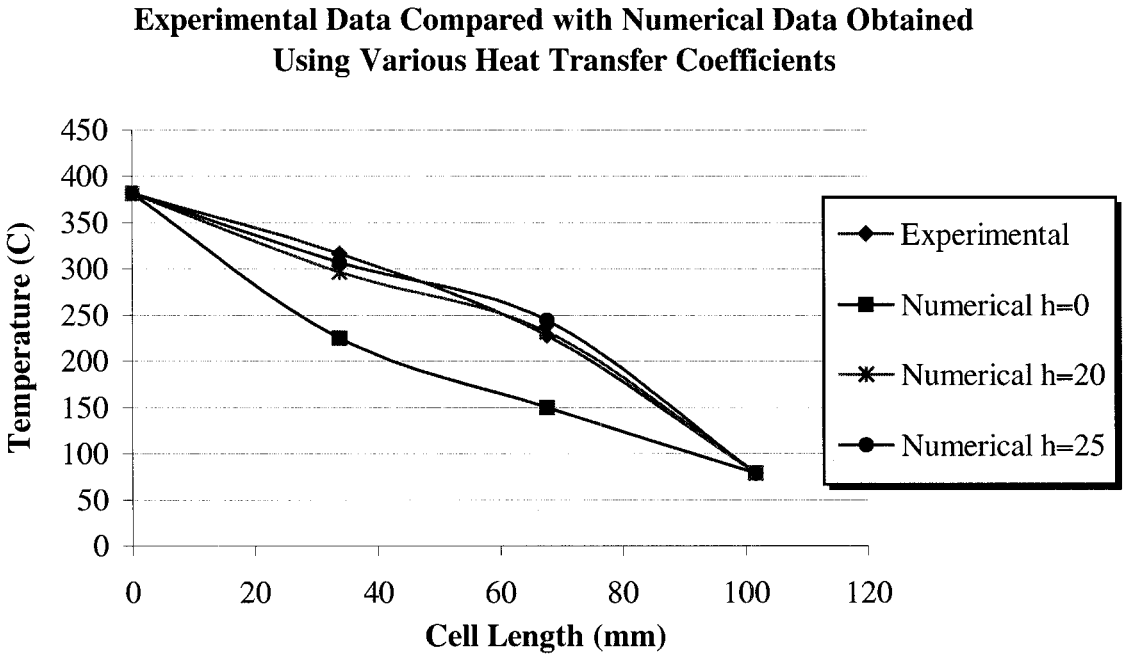

Figure 12. Experimental data compared with numerical data obtained using various heat transfer coefficients for a hot end value of 382°C

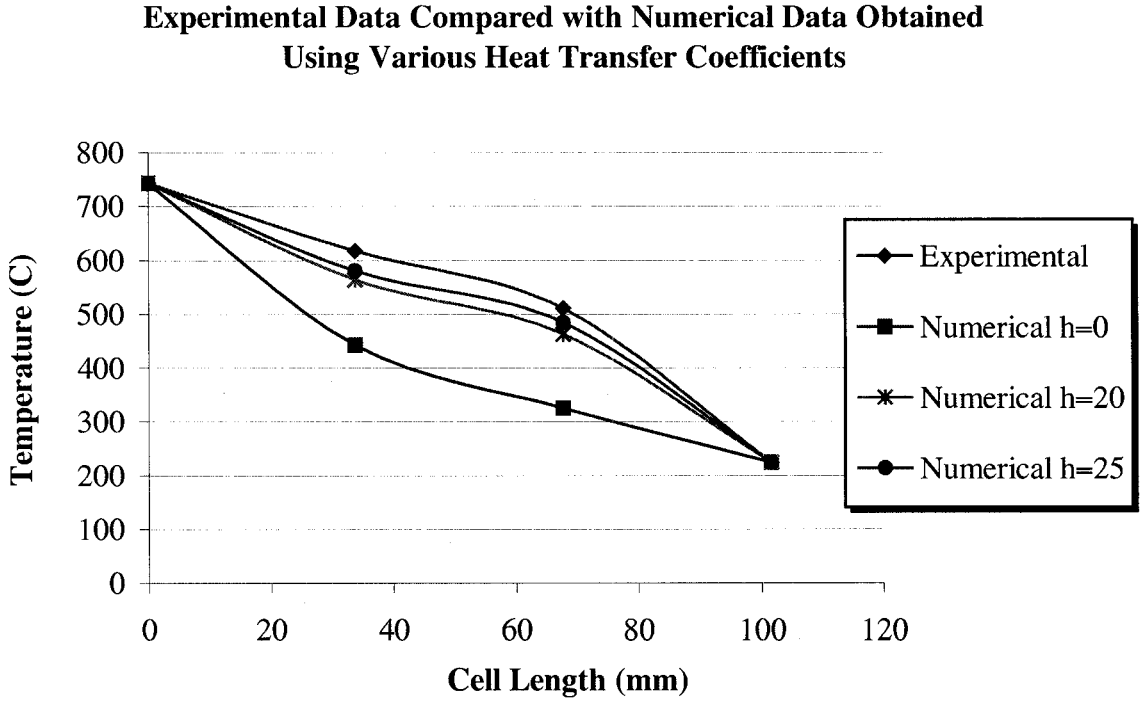

Figure 13. Experimental data compared with numerical data obtained using various heat transfer coefficients for a hot end value of 743°C

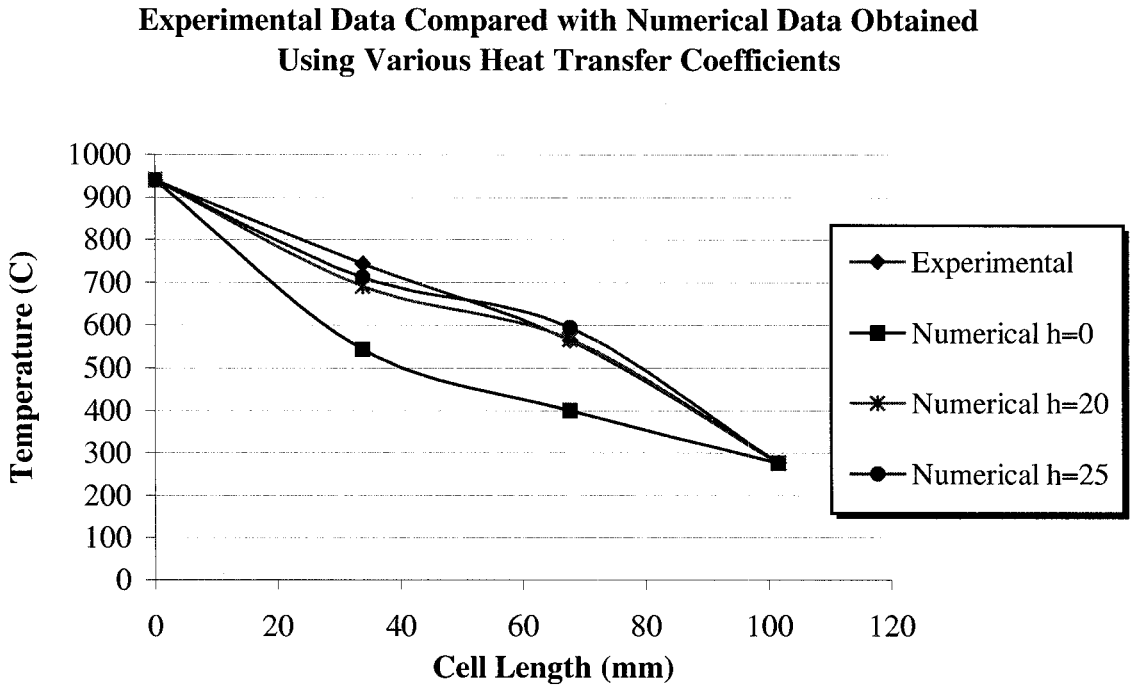

Figure 14. Experimental data compared with numerical data obtained using various heat transfer coefficients for a hot end value of 940°C

Very little work has been done with regards to the heat transfer effects of sodium vapor in the continuum and slip flow regimes. As a result a calculation based on theoretical values could not be made to select an appropriate heat transfer coefficient. However, convection theory suggests that gases at 1 atm subjected to forced convection generally have heat transfer coefficient values between (approximately) 10-300 W/m^2K, while gases under natural convection have heat transfer coefficient values between (approximately) 7-50 W/m^2K [1]. With this in mind, heat transfer coefficient values ranging from 1-25 W/m^2K were input to the model in an effort to yield values more comparable with the experimental results.

The numerical results using heat transfer coefficients of 20 and 25 W/m^2K compared well with the experimental data, and were within the range of heat transfer coefficients of gases at 1 atm for free and forced convection. However, very little work has been done with rarefied heat transfer with sodium, and consequently the values selected for the heat transfer coefficients could not be verified by calculation. Sodium vapor thermo-physical properties such as thermal conductivity and specific heat are not available for a wide range of conditions for the continuum regime, and such data is totally absent for the slip flow regime. The experimental and numerical values obtained in this study verify that internal convection should be taken into consideration when examining the heat transfer affects related to AMTEC cells. These finding will assist members of the AMTEC community in subsequent research efforts regarding cell optimization

Acknowledgements

The work described in this paper was performed at the Jet Propulsion Laboratory, California Institute of Technology, under contract with the National Aeronautics and Space Administration.

Reference herein to any specific commercial product, process, or service by trade name, trademark, manufacturer, or otherwise, does not constitute or imply its endorsement by the United States Government or the Jet Propulsion Laboratory, California Institute of Technology.

The author would like to thank the following individuals for their technical support in the completion of this work: Dr. Virgil Shields, Dr. Roger Williams, Dr. M. A. Ryan, Dr. Mark Underwood, Dr. Robert Richter, Dr, David Klett and Mark Kithcart.

References

1. Bejan, Adrian, Heat Transfer, 1993, John Wiley & Sons, Inc., New York.

2. Huang, Lianmin, Merrill, John M., and Mayberry, Clay, 1998 "Empirical Correlations of the Performance of Vapor-Anode PX-Series AMTEC Cells," 33rd Intersociety Engineering Conference on Energy Conversion, pp. 98-237.

3. Ivanenok III, Joseph F., and Sievers, Robert K., 1995, "AMTEC Radioisotope Power System for the Pluto Express Mission," 30th Intersociety Energy Conversion Engineering Conference, pp. 661-666.

4. Klett, D.E., and Irey, R.K., "Experimental Determination of Thermal Accommodation Coefficients," Adv. In Cryogenic Engineering, v.14, Plenum Press, N.Y. 1969.

5. Merrill, John M., Clark, Matt, and Daigle, Troy 1997, "Test Plan AMTEC PX Series Cells (Draft)," Kirtland AFB, NM, pp.2-11.

6. Mondt, Jack F., 1998, "Space Radioisotope Power Source Requirements Update and Technology Status," 33rd Intersociety Engineering Conference on Energy Conversion, pp. 98-228.

7. Schock, Alfred, Noravian, Heros, and Or, Chuen, 1997, "Coupled Thermal, Electrical, and Fluid Flow Analyses of AMTEC Converters, with Illustrative Application to OSC's Cell Design," 32nd Intersociety Energy Conversion Engineering Conference, pp. A-1-A-9.

8. Schock, A., Noravian, H., Kumar, V., and Or, T., "Suplementary AMTEC Multitube Cell Design Studies," An Orbital Sciences Corporation Report: Orbital Sciences Corporation, 20301 Century Blvd., Germantown, Maryland 20874.

9. Schock, Alfred, Noravian, Heros, Or, Chuen, and Kumar, Vasanth, 1998, "Illustrative Application of AMTEC Cell Analysis with Overpotential Correction, and Predicted Cell Performance for a Wide Range of Design and Operating Parameters," 33rd Intersociety Energy Conversion Engineering Conference, pp.98-243 1-10.

10. Tournier, Jean-Michel, and El-Genk, Mohamed S., 1998, "An Analysis of AMTEC, Multi-Cell Ground Demo for the Pluto/Express Mission," 33rd Intersociety Energy Conversion Engineering Conference, pp. 98-057 1-4.

11. Vining, Cronin B., Williams, Roger M., Underwood, Mark L., Ryan, M. A., and Suitor, Jerry W., "Reversible Thermodynamic Cycle for AMTEC Power Conversion," 1992, 27th Intersociety Energy Conversion Engineering Conference, pp. 3.123-3.127.

12. Advanced Modular Power Systems (AMPS) website, www.ampsys.com.htm, Ann Arbor, MI.

13. Advanced Modular Power Systems (AMPS) website, www.ampsys.com/intro.htm, Ann Arbor, MI.

NOMENCLATURE

AMTEC	Alkali Metal Thermal to Electric Converter
JPL	Jet Propulsion Laboratory
AMPS	Advanced Modular Power Systems
OSC	Orbital Sciences Corporation
BASE	Beta Alumina Solid Electrolyte
Kn	Knudsen Number
P	Sodium Vapor Pressure
λ	Mean Free Path
V	Cell Volume
n	Number of Moles
N	Number of Sodium Vapor Molecules in Cell
R_u	Universal Gas Constant
d	Molecular Diameter of Sodium